

Chaos in neural networks with a nonmonotonic transfer function

D. Caroppo, M. Mannarelli, G. Nardulli, and S. Stramaglia

Dipartimento Interateneo di Fisica and Istituto Nazionale di Fisica Nucleare, Sezione di Bari, via Amendola 173, 70126 Bari, Italy

(Received 23 March 1999)

Time evolution of diluted neural networks with a nonmonotonic transfer function is analytically described by flow equations for macroscopic variables. The macroscopic dynamics shows a rich variety of behaviors: fixed-point, periodicity, and chaos. We examine in detail the structure of the strange attractor and in particular we study the main features of the stable and unstable manifolds, the hyperbolicity of the attractor, and the existence of homoclinic intersections. We also discuss the problem of the robustness of the chaos and we prove that in the present model chaotic behavior is fragile (chaotic regions are densely intercalated with periodicity windows), according to a recently discussed conjecture. Finally we perform an analysis of the microscopic behavior and in particular we examine the occurrence of damage spreading by studying the time evolution of two almost identical initial configurations. We show that for any choice of the parameters the two initial states remain microscopically distinct. [S1063-651X(99)14608-7]

PACS number(s): 87.10.+e, 05.20.-y, 05.45.-a

I. INTRODUCTION

Since the pioneering work by Sompolinsky *et al.* [1], the occurrence of oscillations and chaos has become a major field of interest in the frame of neural networks [2]. Neural networks with symmetric synaptic connections have been the object of extensive studies using methods closely related to those used in the theoretical description of the spin glasses [3], since they admit an energy function. Also asymmetric synapses have been studied and the presence of chaotic dynamics was examined, following [1], in a number of subsequent papers (see, e.g., [4–8]). The investigation of chaotic neural networks is interesting, not only from a theoretical point of view, but also for practical reasons, as their dynamical possibilities are richer and allow for a larger spectrum of engineering applications (see, e.g., Ref. [9]). It is also worth stressing that the brain is a highly dynamic system. The rich temporal structure (oscillations) of neural processes has been studied in [10–13]; chaotic behavior has been discovered in the nervous system [14]. Relying on these neurophysiological findings, the study of chaos in neural networks may be useful in the comprehension of cognitive processes in the brain [15].

Asymmetric synapses are not the only route to chaos in neural networks; another possibility is to use a nonmonotonic functional dependence for the activation function, i.e., the transfer function that gives the state of the neuron as a function of the postsynaptic potential. In recent papers [16,17] it has been shown that such a nonmonotonic transfer function may lead to macroscopic chaos in attractor neural networks: chaos appears in a class of macroscopic trajectories characterized by an overlap of the initial configuration that never vanishes. In other words, the network preserves a memory of the initial configuration, but the macroscopic overlap does not converge to a fixed value and oscillates, giving rise to a chaotic time series. Also the case of diluted networks with dynamical, adaptative synapses and nonmonotonic neurons in presence of a Hebbian learning mechanism has been studied, and it has been found that the adaptation leads to a reduction of dynamics [18].

In this paper we further analyze the dynamic behavior of

attractor neural networks with nonmonotonic transfer function. In particular, we analyze a network by mean-field equations whose macroscopic dynamics can be analytically calculated [19,20]. The time evolution of the macroscopic parameters describing the system is determined by a two-dimensional map that exhibits chaotic behavior and represents in our opinion a nontrivial and interesting example of a nonlinear dynamical system (for recent reviews, see, e.g., [21,22]). In the present work the following issues are considered: the structure and hyperbolicity of the strange attractor, the Hausdorff dimension, and Lyapunov exponents. These are typical analyses of the nonlinear dynamical behavior that we perform in a neural-motivated two-dimensional map in order to achieve a better understanding of the dynamics of this class of neural networks. We also analyze the problem of the fragility of chaos and we explicitly prove that the present model behaves in agreement with the conjecture in [23]; i.e., that periodicity windows are constructed around spine loci (one-dimensional manifolds in the two-dimensional parameter space of the model here considered). This is in our opinion an interesting confirmation of this conjecture that sheds light on the geometrical features of the periodicity windows to be found in the chaotic regions. Finally, we examine the microscopic behavior underlying the mean field description: we consider two replicas of the system starting from slightly different initial conditions and we show that these two different configurations never become identical, independently of their macroscopic behavior. This feature was already observed in diluted networks with a monotonic transfer function [19]; here we prove that such behavior is also present in the case of nonmonotonic neurons. It follows that at the microscopic level the network dynamics is always considered to be chaotic, whereas from a macroscopic, mean field point of view, a rich variety of behaviors can occur: fixed-point, periodicity, and chaos. We note that a similar emergence of a macroscopic evolution in the presence of microscopic chaos has recently been found in another framework, i.e., chaotic coupled map models; and it has been termed *nontrivial collective behavior* (NTCB, see [24], and references therein).

The paper is organized as follows: in the next section the model is described and the flow equations for macroscopic

parameters are reported and analyzed. In Sec. III we study the time evolution of the distance between two replicas of the network. In Sec. IV we present our conclusions.

II. THE MODEL: ANALYSIS OF FLOW EQUATIONS

We consider the model of Ref. [18], i.e., a neural network with N three-state neurons (spins) $s_i(t) \in \{-1, 0, 1\}$, $i = 1, \dots, N$. For each neuron s_i , K input sites $j_1(i), \dots, j_K(i)$ are randomly chosen among the N sites, and NK synaptic interactions J_{ij} are introduced. We assume that the synapses are two-state variables $J_{ij} \in \{-1, 1\}$, randomly and independently sampled with mean J_0 ; they are not assumed to evolve in time (the case of adapting synapses is studied in [18]). A parallel deterministic dynamics is assumed for neurons, where the local field acting on neuron s_i (the postsynaptic potential) is given by

$$h_i(t) = \sum_j J_{ij} s_j(t), \quad (1)$$

with the sum taken over the K input neurons. We assume a nonmonotonic transfer function, depending on the parameter θ [25–29]:

$$s_i(t+1) = F_\theta(h_i(t)), \quad (2)$$

where $F_\theta(x) = \text{sgn}(x)$ when $|x| < \theta$ and vanishes otherwise.

The dynamics of this model is solved by macroscopic flow equations for the parameters describing the system. Let us now introduce order parameters for the neurons. The overlap with pattern $\{\xi\}$ to be retrieved (we choose $\{\xi=1\}$ for simplicity) is measured by $m(t) = \langle s(t) \rangle$. We stress that the suppression of the site index i is possible because all averages are site independent. The neuronal activity is given by $Q(t) = \langle s^2(t) \rangle$. The flow equations for m and Q have been obtained in [18]:

$$m(t+1) = \text{erf}\left(\frac{\mu(t)}{\sqrt{\sigma(t)}}\right) - \frac{1}{2} \left[\text{erf}\left(\frac{\theta + \mu(t)}{\sqrt{\sigma(t)}}\right) - \text{erf}\left(\frac{\theta - \mu(t)}{\sqrt{\sigma(t)}}\right) \right], \quad (3)$$

$$Q(t+1) = \frac{1}{2} \left[\text{erf}\left(\frac{\theta + \mu(t)}{\sqrt{\sigma(t)}}\right) + \text{erf}\left(\frac{\theta - \mu(t)}{\sqrt{\sigma(t)}}\right) \right], \quad (4)$$

where

$$\mu(t) = Km(t)J_0 \quad (5)$$

and

$$\sigma(t) = K(Q(t) - J_0^2 m^2(t)) \quad (6)$$

are mean and variance, respectively, of the local field acting on neurons at time t .

Depending on the value of θ and J_0 , three kinds of dynamic behavior are possible for the network, which lead to a phase diagram [18]. Two fixed-point ordered phases are present, the *ferromagnetic* phase (F) characterized by m

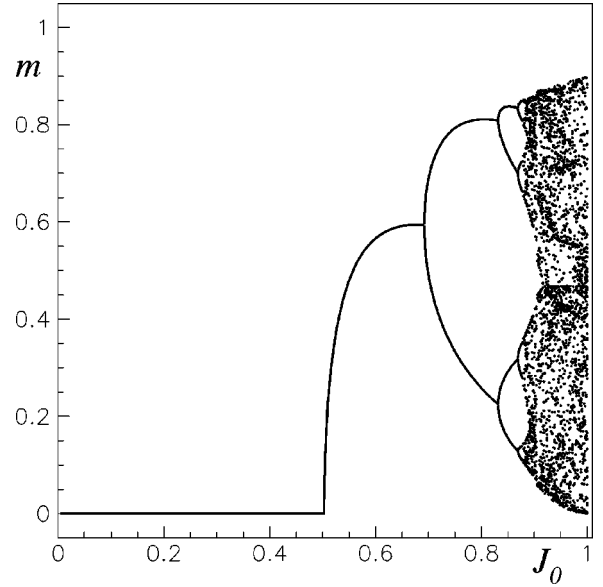


FIG. 1. Bifurcation map of m versus J_0 in the case $K=10$ and $\theta=5$.

>0 , $Q>0$ and the *self-sustained activity* phase (S) characterized by $m=0$, $Q>0$. A phase without fixed points, corresponding to cyclic or chaotic attractors and characterized by $m_i>0$, $Q_i>0$, is also found; we call it the *period-doubling* phase (D). We remark that the phase corresponding to the fixed point ($m=0, Q=0$) is missing in this model. Depending on the values of the parameters, we can get one phase or another; in Fig. 1 the bifurcation diagram of m versus J_0 , while keeping $\theta=5$ fixed, is shown (for $K=10$). The S fixed point is stable for $J_0<0.5$; at $J_0\sim 0.5$ the F fixed point continuously appears and remains stable until $J_0\sim 0.69$, where a bifurcation to a stable 2-cycle takes place. The bifurcation mechanism is *period doubling*; i.e., an eigenvalue of the Jacobian matrix at the fixed point leaves the unitary disk passing through -1 . Increasing J_0 , successive bifurcations arise; eventually the system enters in the chaotic region at $J_0\sim 0.88$. In the chaotic region, windows of periodicity intercalate with chaotic attractors, which is a well-known feature of dynamical systems with chaotic behavior. We have verified that the values of J_0 where the successive bifurcations take place are consistent with Feigenbaum's universality law [30]; i.e., the length in J_0 of the range of stability for an orbit of period 2^n decreases approximately geometrically with n , and the ratio of successive range lengths is close to $4.669\dots$ for large n . We note that, in the phase D , the two-dimensional map [Eqs. (3) and (4)] still possesses the F and S fixed points, but they are unstable.

Let us now consider the strange attractor and its dependence on J_0 . For example, in Fig. 2 the strange attractor is shown, for $\theta=5$ and $K=10$, in correspondence with $J_0=0.9$, 0.95 , and 0.99 , respectively; the fixed point F is represented by a star. In the case $J_0=0.9$, the attractor is made of two disconnected components; in the stationary regime successive points on the attractor jump from one component to the other. As J_0 grows ($J_0=0.95$), the attractor evolves into a more complicated structure, still composed of two disconnected components. We remark that in these two cases the fixed point F is not a limit point of the attractor. At J_0

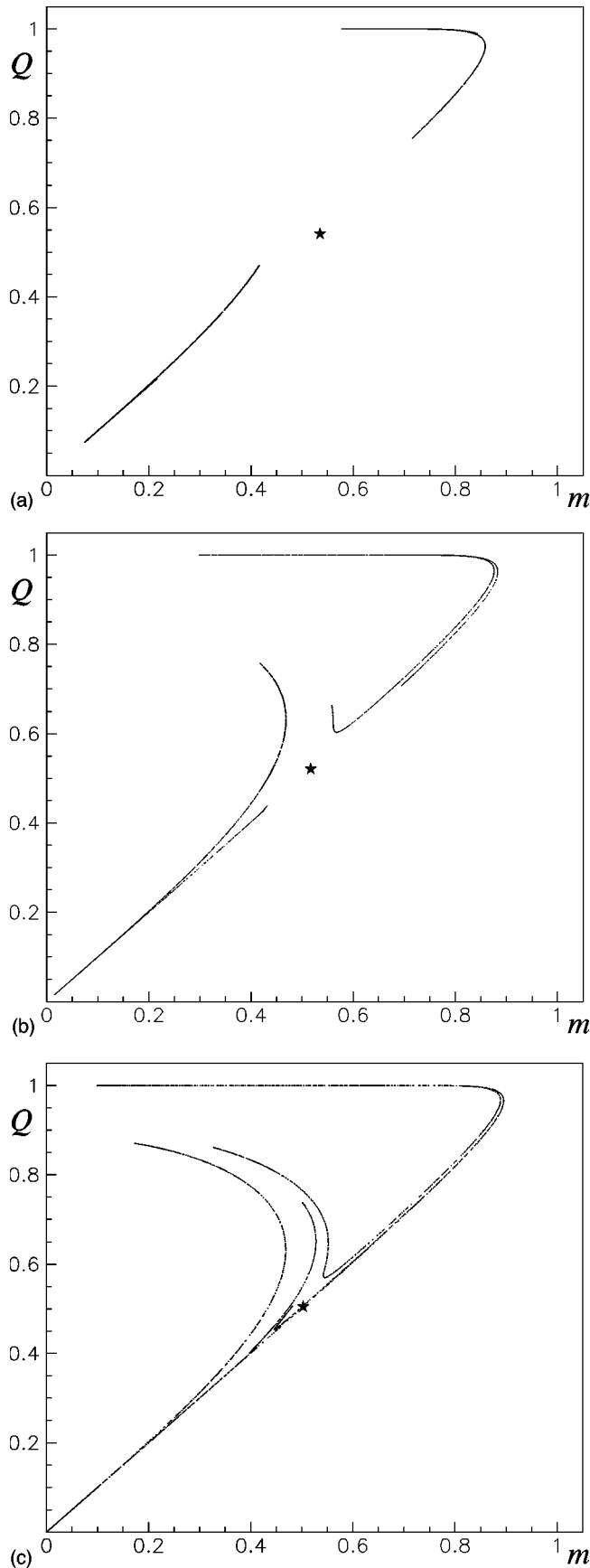


FIG. 2. Strange attractor of the map (3) and (4), corresponding to $K=10$, $\theta=5$, and $J_0=0.9$ (a), 0.95 (b), 0.99 (c). The star represents the fixed point F .

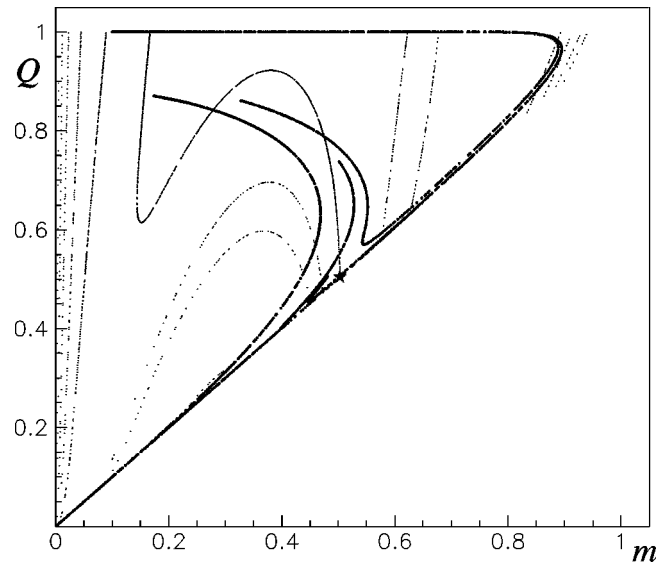


FIG. 3. Stable and unstable manifolds of the fixed point F (represented by the star), for $J_0=0.99$, $K=10$, and $\theta=5$.

$=0.99$ the two components of the attractor merge and F becomes a limit point of the attractor. Concerning the Hausdorff dimension of the attractor, we found it to be close to 0.95 in the three cases described above (the dimension was estimated by the method described in [31]; see also [32]).

Let us now discuss the hyperbolicity of the attractor. We call that in the hyperbolic case many interesting properties about the structure and dynamics of chaos hold (see, e.g., [21,22]). In Fig. 3 we have shown finite length segments of the stable manifold of the fixed point F (for $J_0=0.99$, $\theta=5$, $K=10$); since F is on the attractor, we can argue that the attractor is the closure of the unstable manifold of F . We note that the stable and unstable manifolds have homoclinic intersections. Moreover, Fig. 3 displays near tangencies between the stable and unstable manifolds; it is reasonable that some other segment of the stable manifold will be exactly tangent to the unstable manifold. We conclude, therefore, that the attractor is not hyperbolic (see [21] for a discussion on the nonhyperbolicity of Henon's attractor [33], which has similarities to the attractor of the map considered here).

We continue our analysis of the dynamical properties of the neural model and we turn now to the Lyapunov exponents. By evaluating the Jacobian of the map, we find it to be area contracting; therefore there is one positive Lyapunov exponent at most. We have evaluated the first (λ_1) and the second (λ_2) Lyapunov exponents by the method of Ref. [34], and the results are displayed in Figs. 4(a) and 4(b); as expected, the second Lyapunov exponent is always negative. For a given model, the ratio of the number of free parameters to the number of positive Lyapunov exponents seems to be related, according to a conjecture in [23], to the fragility of chaos: if this ratio is greater or equal to 1 a slight change of the parameters can typically destroy chaos and a stable periodic orbit sets in. Since in our case the ratio is 2 (we have two parameters, J_0 and θ), we conclude that the macroscopic chaos of the model should be fragile. In Fig. 5 a portion of the parameter space is depicted; here black pixels correspond to chaotic attractors and white pixels to stable periodic attractors. One can see that extended periodicity windows are

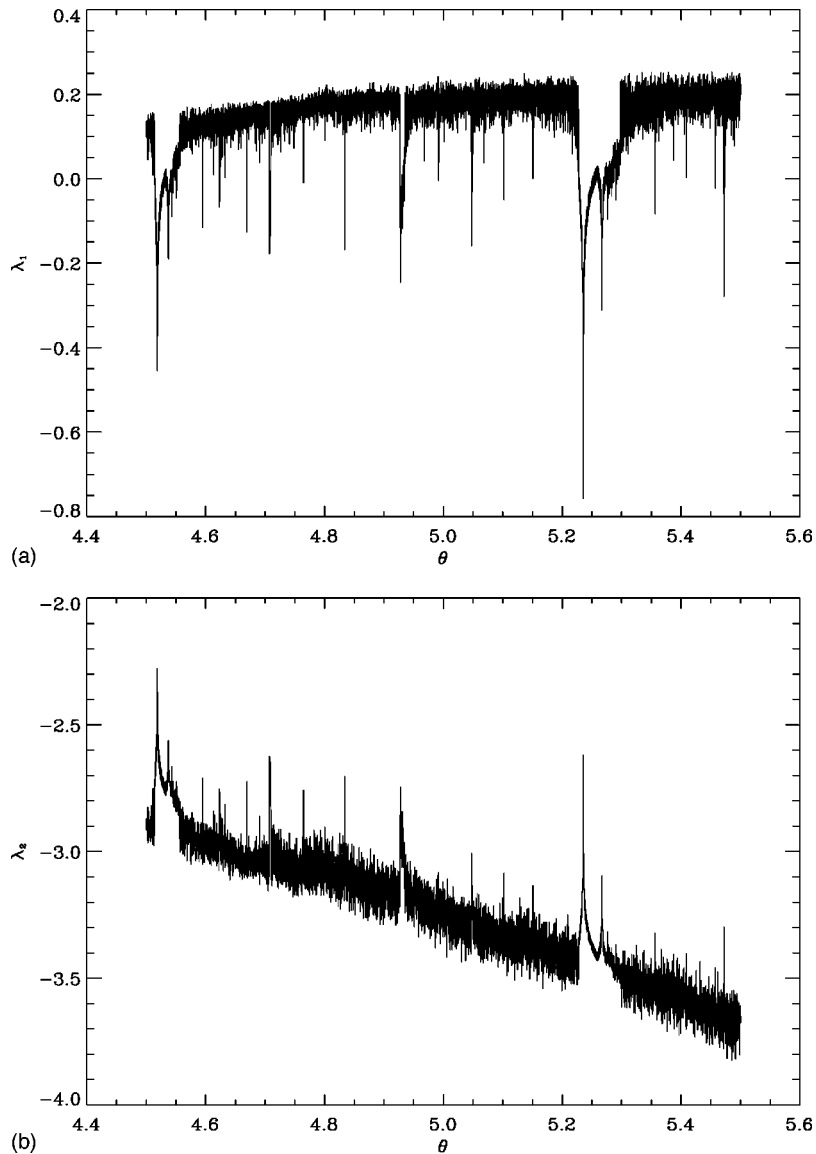


FIG. 4. (a) First and (b) second Lyapunov exponents versus θ , corresponding to $K=10$ and $J_0=0.9$.

present; they are apparently dense everywhere. The above cited conjecture in [23] is based on the idea that periodicity windows are constructed around *spine loci*, i.e., values of the parameters that give rise to superstable orbits. For two-dimensional maps, the spine locus of cycles with period p is determined by the conditions $\det M=0$ and $\text{tr } M=0$, where M is the Jacobian matrix of the p -iterated map. Our map has no critical points (like, e.g., Henon's map) because the determinant of the Jacobian never vanishes; hence the condition $\det M=0$ cannot be strictly satisfied. However, since the map is area contracting, $\det M \sim 0$ for a periodic orbit with sufficiently high period p (see [23]); one can therefore neglect the condition $\det M=0$ and the stability requirements reduce to one condition for stability, which according to the discussion above is $\text{tr } M=0$. It follows that the spines are of codimension 1, i.e., one-dimensional manifolds in the J_0 - θ plane. In Fig. 6 we have shown finite length segments of the spine loci determined by the condition $\text{tr } M=0$ with $p=32, 64$, and 24 . Since we do not have an analytic treatment of the two-dimensional map, we have implemented the condition $\text{tr } M=0$ numerically. White areas are periodicity windows that are apparently constructed around spine loci;

hence the conjecture in [23] is confirmed. We note, in passing, that our findings confirm that the behavior of two-dimensional area-contracting maps is often similar to that of one-dimensional maps with critical points [35].

The concept of robust chaos as associated with an attractor for which the number of positive Lyapunov exponents (in some region of parameter space) is larger than the number of free (accessible) parameters in the model has been also discussed in [36]; recently it has been pointed out that nonmonotonic transfer functions may lead to robust chaos in time series generated by feed-forward neural nets [37]. Probably fully connected networks with a nonmonotonic activation function might provide robust chaos; however, the analytic analysis of these models is difficult since the dynamical theory that describes the fully connected Hopfield model [38] has not yet been extended to the case of nonmonotonic neurons.

III. DAMAGE SPREADING

A system is said to exhibit damage spreading if the distance between two of its replicas, which evolve from slightly

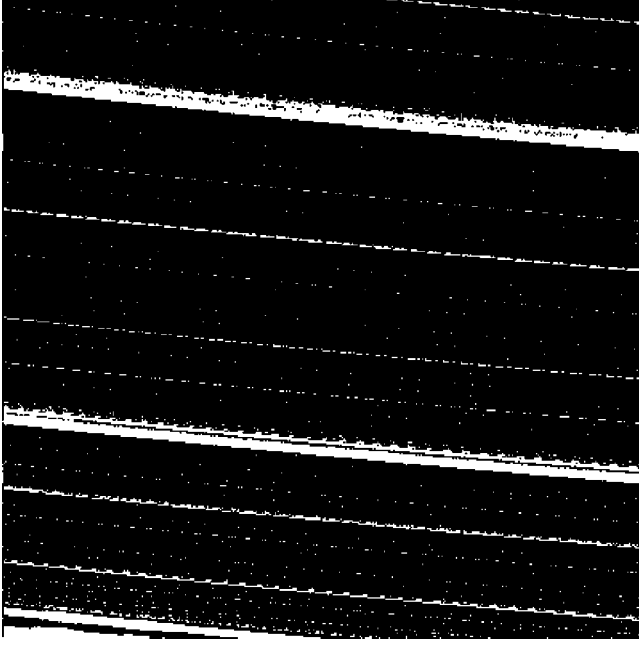


FIG. 5. A portion of the parameter space, $(\theta, J_0) \in [5, 5.12] \times [0.88, 0.9]$. Black pixels correspond to chaotic behavior, whereas white pixels correspond to periodicity.

different initial conditions, increases with time (see, e.g., [39]). Even though damage spreading was first introduced in the context of biologically motivated dynamical systems [40], it has become an important tool for studying the influence of initial conditions on the time evolution of various physical systems. In [19] this phenomenon was studied in diluted networks with a monotonic transfer function. The occurrence of damage spreading in the Little-Hopfield neural networks, both for fully connected and strongly diluted systems, has been studied in [41]. Here we generalize this study to the case of diluted networks with nonmonotonic neurons. Let us consider two replicas of the same system having ini-

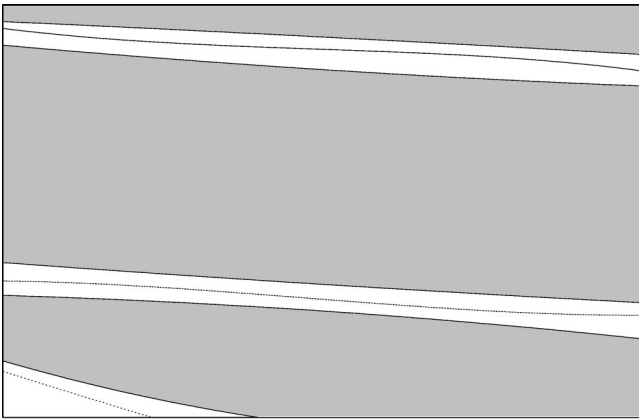


FIG. 6. A portion of parameter space, $(\theta, J_0) \in [5, 5.015] \times [0.88, 0.8825]$. White areas correspond to periodic behavior. The solid line represents the spine locus with $p=24$, the dashed line is the spine locus with $p=64$, and the dotted line is the spine with $p=32$. These curves are obtained numerically by interpolation of a finite set of points characterized by the condition $\text{tr} M=0$. Gray areas correspond to chaotic behavior; they contain infinite periodic windows not displayed here.

tial $t=0$ configurations with the same activity Q_0 and overlap m_0 but microscopically different for a small number of neurons. Subsequently the two replicas evolve, subject to the same dynamics, since their synaptic connections are identical. The two replicas will have the same macroscopic parameters $m(t)$ and $Q(t)$ at every later time t , since the trajectories $m(t)$ and $Q(t)$ are obtained by m_0 and Q_0 iterating equations (3) and (4). At the microscopic level the situation may be different, and we therefore study a suitably defined distance between the two replicas. Let us call $h^1(t)$ and $h^2(t)$ the local fields acting on s^1 and s^2 , two corresponding neurons of the replicas located on the same lattice site. The distance between the local fields is defined by

$$d(t) = \langle [h^1(t) - h^2(t)]^2 \rangle = 2[\sigma(t) - \Delta(t)], \quad (7)$$

where

$$\Delta(t) = \langle h^1(t)h^2(t) \rangle - \langle h^1(t) \rangle \langle h^2(t) \rangle \quad (8)$$

is the linear correlation between local fields at time t . In the limit $N \rightarrow \infty$ with K large and finite, h^1 and h^2 can be treated as Gaussian variables with probability density:

$$P_t(h^1, h^2) = \frac{1}{C} \exp \left\{ -\frac{1}{2} \left[\frac{\sigma}{\sigma^2 - \Delta^2} [(h^1 - \mu)^2 + (h^2 - \mu)^2] - \frac{2\Delta}{\sigma^2 - \Delta^2} (h^1 - \mu)(h^2 - \mu) \right] \right\}, \quad (9)$$

where C is a normalization factor and σ , μ , Δ are implicitly dependent on time t . The time evolution law for $\Delta(t)$ is given by

$$\Delta(t+1) = K(\langle s^1(t+1)s^2(t+1) \rangle - J_0^2 m^2(t+1)). \quad (10)$$

The average of the product of corresponding neurons in the two replicas is evaluated as follows:

$$\langle s^1(t+1)s^2(t+1) \rangle = \int dh^1 \int dh^2 P_t(h^1, h^2) F_\theta(h^1) F_\theta(h^2); \quad (11)$$

the evaluation of the integral on the right-hand side of Eq. (11) is straightforward and leads to the time evolution law for $\Delta(t)$, which can be written as follows:

$$\Delta(t+1) = K \left(\int_{-\mu/\sqrt{\sigma}}^{(\theta-\mu)/\sqrt{\sigma}} Dz I(z) - \int_{-(\theta+\mu)/\sqrt{\sigma}}^{-\mu/\sqrt{\sigma}} Dz I(z) - J_0^2 m^2(t+1) \right), \quad (12)$$

where $Dz = e^{-(1/2)z^2} (dz/\sqrt{2\pi})$ is the Gaussian measure and

$$I(z) = \text{erf}(A) + \frac{1}{2} [\text{erf}(B) - \text{erf}(C)], \quad (13)$$

with

$$A = \frac{\mu\sqrt{\sigma}}{\sqrt{\sigma^2 - \Delta^2}} + \frac{\Delta z}{\sqrt{\sigma^2 - \Delta^2}}, \quad (14)$$

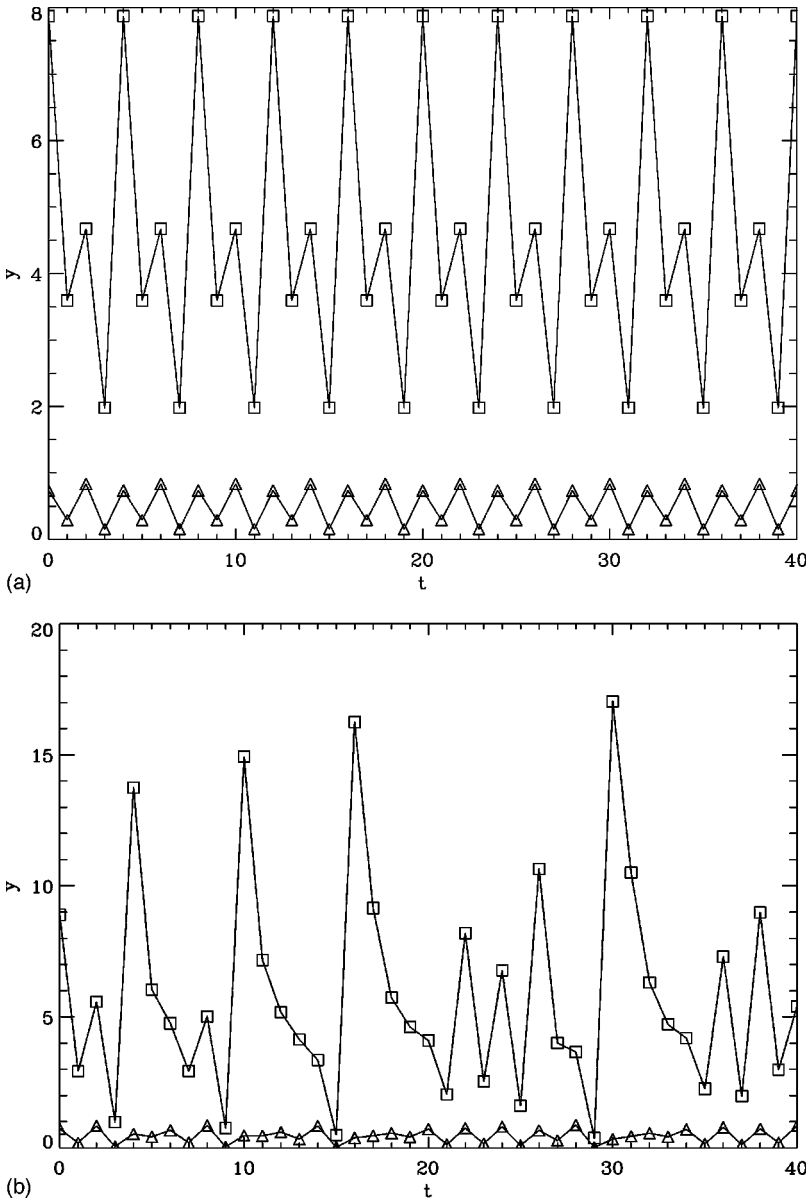


FIG. 7. Stationary regime of the distance between two configurations having initial distance $d(0) = 10^{-5}$. Squares correspond to the distance, $y = d(t)$, while triangles represent the overlap, $y = m(t)$. The parameter values are (a) $K = 10$, $\theta = 5$, and $J_0 = 0.85$; and (b) $K = 10$, $\theta = 5$, and $J_0 = 0.95$.

$$B = \frac{(\theta - \mu)\sqrt{\sigma}}{\sqrt{\sigma^2 - \Delta^2}} - \frac{\Delta z}{\sqrt{\sigma^2 - \Delta^2}}, \quad (15)$$

$$C = \frac{(\theta + \mu)\sqrt{\sigma}}{\sqrt{\sigma^2 - \Delta^2}} + \frac{\Delta z}{\sqrt{\sigma^2 - \Delta^2}}. \quad (16)$$

Equation (12), together with Eqs. (3) and (4), solves the time evolution of $\Delta(t)$. We remark that $\Delta(t) = \sigma(t)$ [i.e., $d(t) = 0$] is a fixed point for Eq. (12). The possible occurrence of damage spreading can be now seen to be equivalent to the instability of the fixed point $\Delta = \sigma$. We have studied this problem numerically. We find that damage spreading occurs for any choice of the parameters J_0 , θ , K . It follows that, from a microscopic point of view, the motion of the system is always to be considered chaotic, even though at the macroscopic level it can exhibit different behaviors (fixed-point, periodicity, chaos). In Fig. 7 we depict the stationary regime of $d(t)$ in the case of periodic macroscopic dynamics and chaotic dynamics; the initial distance was $d(0) = 10^{-5}$. The macroscopic behavior can be seen in the lower part of

the figures [the overlap trajectory $m(t)$]; it is a cycle with period 4 in case (a) and is chaotic in case (b). Correspondingly, the distance $d(t)$ is always greater than zero (i.e., damage spreading occurs) and has period 4 in case (a), whereas it shows chaotic behavior in case (b).

We remark that in Ref. [18] it has been shown that the presence of adapting synapses in these networks leads to reduction of macroscopic dynamics. The adapting system self-regulates its synaptic configuration, by its own dynamics, so as to escape from chaotic regions: in the stationary regime, the mean of synapses $J(t)$ remains practically constant (equal to the stationary value J_{stat}) and the system settles into periodic macroscopic orbits. Since we found damage spreading for all fixed values of J_0 , it follows that the adapting system also displays damage spreading in the stationary regime. In other words, the adaptiveness of synapses should not remove damage spreading, although it reduces the macroscopic dynamics. However, damage spreading may be suppressed if the neuron updating rule becomes stochastic by a proper amount of noise (the two replicas being subject to the same noise; see [7,39,41]).

IV. CONCLUSIONS

In this paper we have studied a diluted neural network with a nonmonotonic activation function, whose macroscopic dynamics is given by a two-dimensional map. Some properties of this nonlinear map have been studied: the structure and nonhyperbolicity of the strange attractor. In particular, we have analyzed the fragility of the chaos and we have shown the validity of a recently discussed conjecture; i.e., periodicity windows are constructed around spine loci. Finally we have studied the time evolution of the distance between two replicas of the model that evolve subject to the

same synaptic configuration. We have found that the two replicas never become identical, and the system exhibits damage spreading for any choice of parameters. In the stationary regime the distance between the two replicas does not vanish and the trajectory $d(t)$ behaves in agreement with the macroscopic dynamics: it is periodic (chaotic) if $m(t)$ is periodic (chaotic).

ACKNOWLEDGMENTS

The authors gratefully thank L. Angelini, G. Gonnella, M. Pellicoro, and M. Villani for useful discussions.

-
- [1] H. Sompolinsky, A. Crisanti, and H. J. Sommers, *Phys. Rev. Lett.* **61**, 259 (1988).
 - [2] D. J. Amit, *Modeling Brain Function* (Cambridge University Press, Cambridge, England, 1989); J. Hertz, A. Krogh, and R. Palmer, *Introduction to the Theory of Neural Computation* (Santa Fe Institute, Santa Fe, NM, 1990).
 - [3] K. H. Fisher and J. A. Hertz, *Spin Glasses* (Cambridge University Press, Cambridge, England, 1991).
 - [4] B. Tirozzi and M. Tsodyks, *Europhys. Lett.* **14**, 727 (1991).
 - [5] B. Doyon, B. Cessac, M. Quoy, and M. Samuelides, *Int. J. Bifurcation Chaos* **3**, 279 (1993).
 - [6] B. Cessac, B. Doyon, M. Quoy, and M. Samuelides, *Physica D* **74**, 24 (1994).
 - [7] L. Molgedey, J. Schuart, and H. G. Schuster, *Phys. Rev. Lett.* **69**, 3717 (1992).
 - [8] C. N. Laughton and A. C. C. Coolen, *J. Phys. A* **27**, 8011 (1994).
 - [9] M. W. Hirsch, *Neural Networks* **2**, 331 (1989).
 - [10] R. Eckhorn, R. Bauer, W. Jordan, M. Brosch, M. Kruse, M. Munk, and H. J. Reitboeck, *Biol. Cybern.* **60**, 121 (1988).
 - [11] C. M. Gray, P. Koenig, A. K. Engel, and W. Singer, *Nature (London)* **338**, 334 (1989).
 - [12] M. Steriade, D. A. McCormick, and T. J. Sejnowski, *Science* **262**, 679 (1993).
 - [13] J. P. Welsh, E. J. Lang, I. Sugihara, and R. R. Llinas, *Nature (London)* **374**, 453 (1995).
 - [14] A. Babloyantz, C. Nicolis, and J. M. Salazar, *Phys. Lett. A* **111**, 152 (1985).
 - [15] C. A. Skarda and W. J. Freeman, *Behav. Brain Sci.* **10**, 161 (1987); W. J. Freeman, *Sci. Am.* **264** (3), 34 (1991).
 - [16] D. Bollè and B. Vinck, *Physica A* **223**, 293 (1996).
 - [17] D. R. C. Dominguez, *Phys. Rev. E* **54**, 4066 (1996).
 - [18] D. Caroppo and S. Stramaglia, *Phys. Lett. A* **246**, 55 (1998).
 - [19] B. Derrida, E. Gardner, and A. Zippelius, *Europhys. Lett.* **4**, 167 (1987).
 - [20] G. Lattanzi, G. Nardulli, G. Pasquariello, and S. Stramaglia, *Phys. Rev. E* **56**, 4567 (1997).
 - [21] E. Ott, *Chaos in Dynamical Systems* (Cambridge University Press, Cambridge, England, 1993).
 - [22] D. K. Arrowsmith and C. M. Place, *Introduction to Dynamical Systems* (Cambridge University Press, Cambridge, England, 1990).
 - [23] E. Barreto, B. R. Hunt, C. Grebogi, and J. A. Yorke, *Phys. Rev. Lett.* **78**, 4561 (1997).
 - [24] A. Lemaitre and H. Chatè, *Phys. Rev. Lett.* **80**, 5528 (1998).
 - [25] K. Kobayashi, *Network* **2**, 237 (1991).
 - [26] P. De Felice, C. Marangi, G. Nardulli, G. Pasquariello, and L. Tedesco, *Network* **4**, 1 (1993).
 - [27] G. Boffetta, R. Monasson, and R. Zecchina, *J. Phys. A* **26**, L507 (1993).
 - [28] R. Monasson and D. O'Kane, *Europhys. Lett.* **27**, 85 (1994).
 - [29] G. J. Bex, R. Serneels, and C. Van den Broeck, *Phys. Rev. E* **51**, 6309 (1995).
 - [30] M. J. Feigenbaum, *J. Stat. Phys.* **19**, 25 (1978).
 - [31] P. Grassberger and I. Procaccia, *Physica D* **9**, 189 (1983).
 - [32] J. P. Eckmann and D. Ruelle, *Rev. Mod. Phys.* **57**, 617 (1985).
 - [33] M. Henon, *Commun. Math. Phys.* **50**, 69 (1976).
 - [34] A. Wolf, J. B. Swift, H. L. Swinney, and J. A. Vastano, *Physica D* **16**, 285 (1985).
 - [35] J. A. Yorke, C. Grebogi, E. Ott, and L. Tedeschini-Lalli, *Phys. Rev. Lett.* **54**, 1095 (1984).
 - [36] S. Banerjee, J. A. Yorke, and C. Grebogi, *Phys. Rev. Lett.* **80**, 3049 (1998).
 - [37] A. Priel and I. Kanter, *Phys. Rev. E* **59**, 3368 (1999).
 - [38] A. C. C. Coolen and D. Sherrington, *Phys. Rev. Lett.* **71**, 3886 (1993).
 - [39] B. Derrida, in *Fundamental Problems in Statistical Mechanics VII*, edited by H. van Beijeren (Elsevier Science, New York, 1990).
 - [40] S. A. Kauffman, *J. Theor. Biol.* **22**, 437 (1969).
 - [41] P. De Felice, C. Marangi, G. Nardulli, and G. Pasquariello, *J. Phys. A* **27**, 4115 (1994).